

Interactions on Nuclei^{*,+}

Paul Hoyer

Nordita
Copenhagen, Denmark

Abstract

I review hard photon initiated processes on nuclei. The space-time development of the DIS reaction as viewed in the target rest frame qualitatively describes the nuclear shadowing of quark and gluon distributions, although it may be difficult to understand the very weak Q^2 dependence of the low x data. The current jet hadron energy distribution at large ν is accurately independent of the target size even at very small energy fractions $z \simeq 0.05$. Color transparency is verified for vector meson (J/ψ , ρ) production, but remains enigmatic in quasiexclusive proton knockout processes. I emphasize the importance of understanding short-range correlations in nuclei, as manifested by subthreshold production and cumulative $x > 1$ DIS processes.

Résumé

1. Introduction

The nucleus is a weakly bound (non-relativistic) state of protons and neutrons. It would therefore appear that a hard scattering process such as deep inelastic lepton scattering (DIS), with a coherence length $1/Q \ll 1$ fm, should give equivalent results for nuclear and free nucleon targets. This view is false, as first demonstrated by the EMC collaboration [1] in 1982. Their data showed that the structure function of an iron nucleus is not simply related to that of deuterium.

The EMC result led to a flurry of experimental and theoretical activity, as documented in the comprehensive review of nuclear effects in structure functions by Arneodo [2]. Today we know that the nuclear structure function is not proportional to the nucleon one, $F_2^A(x) \neq AF_2^N(x)$, for most values of the Bjorken scaling variable $x = Q^2/2m_N\nu$, where Q^2 is the invariant momentum transfer squared and ν is the energy of the

photon in the target rest frame. A compilation of newly reanalysed data from SLAC [3] and NMC [4] is shown in figure 1, and a conventional nomenclature for the observed nuclear effects is given in table 1.

| F_2^A/AF_2^N | x -range | Nuclear effect |
|----------------|---------------------|-------------------|
| < 1 | $x \leq 0.05$ | Shadowing |
| > 1 | $.1 \leq x \leq .2$ | Anti-shadowing |
| < 1 | $.3 \leq x \leq .8$ | EMC effect |
| > 1 | $.8 \leq x \leq 1$ | Fermi motion |
| ∞ | $1 < x \leq A$ | Cumulative effect |

Table 1. Nomenclature of nuclear effects.

The underlying reason for the interesting properties of nuclei as measured in DIS is that their nucleon constituents are relativistic bound states with a rich internal structure of their own, which is resolved by the high Q^2 photons. The data implies that this nucleon structure is modified by the nuclear environment. It should be stressed that the deviation of the ratio F_2^A/AF_2^N from unity is typically less than 20...30%

* Review talk given at the Workshop on Deep Inelastic scattering and QCD, Paris, April 1995

+ NORDITA - 95/65 P

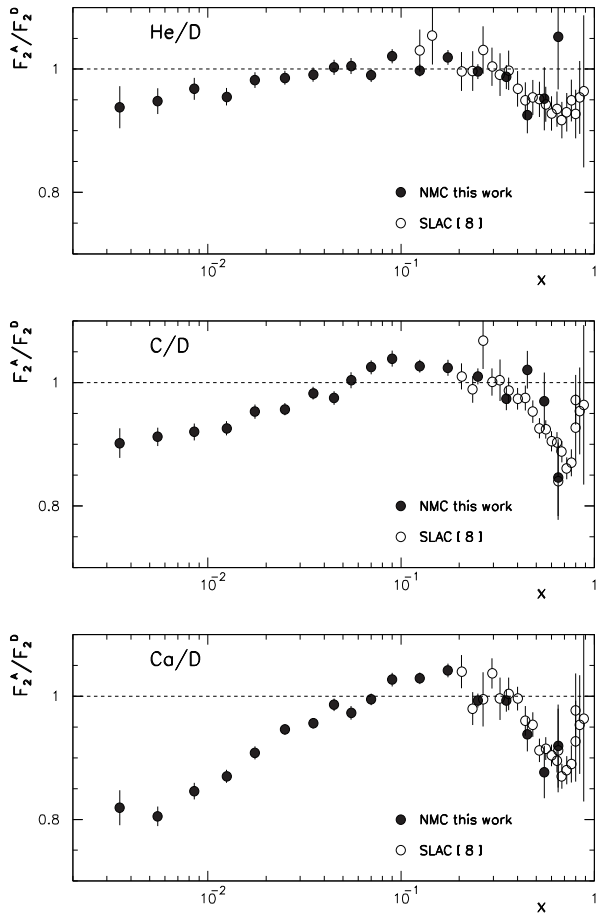


Figure 1. *Compilation [4] of data on the ratio of nuclear to deuterium structure functions for He, C and Ca targets.*

even for large A [2]. The gross features of the nuclear parton distributions are thus similar to the nucleon ones, as expected.

Hence the quark distributions measured by DIS support the standard knowledge that a nucleus may, to a first approximation, be viewed as a collection of weakly bound nucleons.

General arguments exist for the origin of the nuclear effects seen at small x (shadowing, see below), and it is also clear that there will be important effects at large values of x (Fermi motion, cumulative effects). There is still no consensus about the correct explanation of the EMC effect proper, namely the suppression of the nuclear structure function for $.3 \leq x \leq .8$. Models have been proposed [2] both from a hadronic (pions, nuclear binding) and a partonic (confinement radius, quark clusters) point of view. These two approaches are in principle complementary, but in practice their relation to each other is unclear. Since the DIS measurement is highly inclusive (all partons except the observed quark are averaged over) the data does not

readily discriminate between the various proposals. A deeper understanding requires comparisons of the model predictions also with less inclusive measurements of the nuclear wave function.

It should be kept in mind that the nuclear effects observed in DIS are for ‘average’ nuclear configurations, which dominate in the structure function. It is possible that the nuclear effects are much larger if rare Fock states of the constituent nucleons are selected. For example, the ‘cumulative’ $x > 1$ region is kinematically accessible only in the case of nuclear targets.

In this review I discuss some recent topics involving hard lepton scattering on nuclear targets, from the point of view of a particle physicist. I shall argue the case that such reactions can provide new insight on fundamental processes from two principal points of view, as discussed in section 2. In section 3 I review the space-time picture of DIS in the target rest frame, and discuss some developments since the review [2]. Nuclear effects on quark jet hadronization are covered in section 4, and in section 5 I discuss color transparency. Section 6 is devoted to rare, high density fluctuations in nuclei.

A quantitative treatment of nuclear effects generally requires detailed nuclear modelling, the validity of which is difficult for a particle physicist to assess. Here I shall mainly emphasize general, model-independent trends, and refer to the original papers for the motivations of specific assumptions.

2. The two uses of nuclear targets

It is helpful to note that hard interactions in nuclei can be used in two complementary ways, either to give information about the time evolution of the produced states, or to investigate the properties of the nucleus itself.

2.1. The nucleus as a femtovertex detector

The nucleus may (ideally) serve as the smallest conceivable vertex detector. Following (or preceding) a hard collision on a quark or gluon in the nucleus, the rest of the nucleus serves as a medium for detecting secondary interactions of the produced partons. Examples are the hadronization of the recoil quark in DIS (section 4), and the propagation of the $q\bar{q}$ state in $eA \rightarrow e\rho A$ (section 5.1). The usefulness of the femtodetector depends on how well it can be calibrated, i.e., on our understanding of the secondary interactions. I shall discuss below some general features - more will be learnt in future experimental and theoretical studies.

2.2. Study of rare nuclear configurations

Hard interactions on nuclei may be used to study short range correlations in the nuclear wave function. In this case the nucleus is the object of study rather than the detector. For structures much smaller than 1 fm we are in the domain of perturbative QCD and should be able to calculate the probability of rare, shortlived nuclear configurations starting from the longlived ones. An example is provided by the ‘cumulative’ ($x > 1$) region of DIS, where several nucleons deliver their momentum to a single quark or other compact partonic subsystem (section 6).

2.3. Combinations of the above two uses of the nucleus

Sometimes we wish to make a combined use of the nucleus, selecting a rare short-range nuclear configuration and then using the rest of the nucleus as a detector (analogously to what was done in bubble chambers). An example of this is quasielastic ep scattering in a nucleus, observed through the nucleon knock-out reaction $eA \rightarrow ep(A-1)$. This process is of considerable interest for studying color transparency (section 5.4). The struck constituent proton is selected to be in a rare, compact configuration, whereas the remainder of the nucleus serves to measure the rescattering cross section of this ‘small proton’. An essential assumption needed for a color transparency interpretation is that the probability to find the small-sized proton is independent of the nuclear size A .

3. The space-time picture of high energy scattering

The general features of the time development of high energy eA scattering can be established using only Lorentz invariance and the uncertainty principle. For understanding the specifically nuclear effects it is best to view the scattering in the target rest frame, where we have an intuitive understanding of nuclear structure.

The incoming physical electron state (see figure 2) can, at a given instant of time, be expanded in terms of its (bare) Fock states

$$|e\rangle_{phys} = \psi_e |e\rangle + \psi_{e\gamma} |e\gamma\rangle + \psi_{eq\bar{q}} |eq\bar{q}\rangle + \dots \quad (1)$$

The amplitudes ψ_i depend on the kinematic variables describing the states $|i\rangle$, and have a time dependence $\exp(-iE_i t)$, where $E_i = \sum_i \sqrt{m_i^2 + \vec{p}_i^2}$ is the free (kinetic) energy of the partons. (Note that since the Fock expansion is at a fixed time t , energy is not conserved and E_i differs from E_e , the energy of the physical electron.) The ‘lifetime’ $\tau_i \simeq 1/(E_i - E_e)$ of a Fock state $|i\rangle$ is given by the time interval after which the

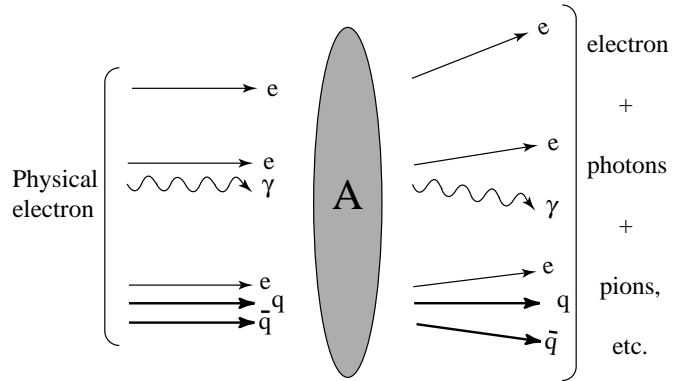


Figure 2. Space-time picture of eA scattering. Three Fock states, $|e\rangle$, $|e\gamma\rangle$ and $|eq\bar{q}\rangle$ are shown to scatter elastically at high energy.

relative phase $\exp[-i(E_i - E_e)]$ is significantly different from unity. There is a continuous mixing of Fock states, with state $|i\rangle$ mixing at a rate $1/\tau_i$.

At high electron energies E_e the lifetimes $\tau_i \propto E_e$ are dilated by the Lorentz factor. If $|i\rangle$ contains partons of mass m_j , energy fraction x_j and transverse momenta $p_{\perp j}$ we have explicitly

$$E_i - E_e \simeq \frac{1}{2E_e} \left(\sum_j \frac{m_j^2 + p_{\perp j}^2}{x_j} - m_e^2 \right) \quad (2)$$

In typical soft collisions the Fock states in Eq. (1) form long before the electron arrives at the nucleus, and they live long after their passage. There is no time within the nucleus to form a new Fock state (*e.g.*, by radiating a gluon), unless its lifetime is of the order of the nuclear radius, $\tau \lesssim R_A$. Hence the scattering inside the nucleus typically is *diagonal* in the Fock basis: $|e\rangle \xrightarrow{A} |e\rangle$, $|e\gamma\rangle \xrightarrow{A} |e\gamma\rangle$, and so on, as indicated in figure 2.

The transverse velocities $v_{\perp j} = p_{\perp j}/x_j E_e$ are typically small at large E_e . Hence the impact parameters (transverse coordinates) of all partons are preserved.

The only effect of the nucleus on the Fock states is then to impart transverse momenta via elastic scattering. This is enough to upset the delicate balance in the electron Fock state mixing so that the asymptotic state which emerges (long after nuclear traversal) can contain a shower of photons and hadrons.

3.1. DIS as seen in the target rest frame

In hard collisions such as deep inelastic scattering, where the momentum transfer is commensurate with the incoming energy, the reaction times are short and the above picture needs to be refined. The usual interpretation of DIS as a measurement of the target

structure functions is simple in the frame where also the target has high momentum (or, equivalently, in terms of light cone coordinates). The nuclear target effects, on the other hand, are easier to discuss in the nuclear rest frame [5, 6, 7, 8].

Deep inelastic scattering $eA \rightarrow e+X$ is characterized by a large electron energy loss ν (in the target rest frame) and an invariant momentum transfer $q^2 = -Q^2$ between the incoming and outgoing electron such that $x = Q^2/2m_N\nu$ is fixed. In terms of Fock states, the electron first emits a photon ($|e\rangle \rightarrow |e\gamma\rangle$) with $E_\gamma = \nu$ and $p_{\perp\gamma}^2 = Q^2(1 - \nu/E_e)$. The energy difference

$$E_{e\gamma} - E_e = \frac{Q^2}{2\nu} = m_N x \quad (3)$$

is *fixed* in the Bjorken limit, implying that the $|e\gamma\rangle$ state typically travels a distance

$$2L_I = \frac{2\nu}{Q^2} = \frac{1}{m_N x} = \begin{cases} 1 \text{ fm} & \text{for } x = .2 \\ 200 \text{ fm} & \text{for } x = .001 \end{cases} \quad (4)$$

defined as two ‘Ioffe lengths’ [5] L_I . The factor two is conventional, and motivated by the fact that the photon still splits into a $q\bar{q}$ pair before interacting in the nucleus: $|e\gamma\rangle \rightarrow |e q\bar{q}\rangle$. If the antiquark \bar{q} carries a fraction α of the photon energy, this transition involves another energy difference

$$E_\gamma - E_{q\bar{q}} = \frac{1}{2\nu} \frac{m_q^2 + p_{\perp q}^2}{\alpha(1-\alpha)} = \mathcal{O}(Q^2/2\nu) \quad (5)$$

which should be as big as the previous one, Eq. (3), to have time to happen during the life-time of the $e\gamma$ state. There are two principal ways in which the large energy difference indicated in Eq. (5) can arise.

3.1.1. Parton model regime

$$\alpha = \mathcal{O}(1/Q^2), \quad p_{\perp q} = \mathcal{O}(\Lambda_{QCD}) \quad (6)$$

The energy of the \bar{q} is finite in the target rest frame†: $\alpha\nu = \mathcal{O}(1/x)$. Its transverse velocity $v_\perp(\bar{q}) = p_{\perp q}/\alpha\nu = \mathcal{O}(x)$, hence during the life-time of the $q\bar{q}$ state it expands a transverse distance

$$r_\perp(q\bar{q}) = v_\perp L_I = \mathcal{O}(1 \text{ fm}) \quad (7)$$

provided $m_q \lesssim \Lambda_{QCD}$.

Depending on the value of x , the asymmetric $q\bar{q}$ pair is created either (a) in the nucleus ($x \gtrsim 0.1$, $L_I \lesssim 1 \text{ fm}$) or (b) well before the nucleus ($x \lesssim 0.01$, $L_I \gtrsim 10 \text{ fm}$). The antiquark interacts in the nucleus with a large cross-section, as dictated by its large transverse spread in Eq. (7). In case (a) $\sigma_{DIS}(eA) \propto A$ while in case (b)

† Equivalently, we may have $1 - \alpha = \mathcal{O}(1/Q^2)$ and a finite quark energy.

the \bar{q} scatters on the nuclear surface and $\sigma_{DIS}(eA) \propto A^{2/3}$. In either case the fast bare quark begins to radiate soft gluons and hadronize only well after the nucleus. In higher orders of $\alpha_s(Q^2)$ the quark may radiate hard gluons before or inside the nucleus, but this radiation is independent of the nucleus and hence does not change the A-dependence of $\sigma_{DIS}(eA)$. To leading order in $1/Q^2$ the fast quark only experiences soft elastic scattering in the nucleus (*cf.* figure 2).

3.1.2. *Gluon scattering regime* The other possibility of achieving a large energy difference in Eq. (5) is

$$\alpha = \mathcal{O}(1/2), \quad p_{\perp q} = \mathcal{O}(Q) \quad (8)$$

Now the quark and antiquark share the photon energy roughly equally. The transverse velocity is $v_\perp = \mathcal{O}(Q/\nu) = \mathcal{O}(x/Q)$, implying a small transverse size of the pair, $r_\perp(q\bar{q}) = \mathcal{O}(1/Q)$. The quark pair has a small interaction cross section in the nucleus, but may (within the lifetime of the pair, and at the price of a coupling constant $\alpha_s(Q^2)$) interact by emitting a gluon of energy fraction $\mathcal{O}(1/Q^2)$. At small x , the gluon is created before arrival at the nucleus and scatters off the nuclear surface, which again results in shadowing. If one assumes that the scattering cross section for a gluon on the nucleus is larger than that of an (anti)quark, this would imply that the shadowing effect is larger in this regime than in the parton model case (6). So far there is little direct experimental information available on the shadowing of the gluon structure function.

It is important to notice that the wee (anti)quark in case (6) and the wee gluon in case (8) have finite momenta of $\mathcal{O}(1/x)$ in the target rest frame. This makes it possible that they are interpreted as belonging to the target wave function in the more familiar frame where the target has large momentum. The parton subprocesses corresponding to cases (6) and (8) are then $\gamma^* q \rightarrow q$ and $\gamma^* g \rightarrow q\bar{q}$, respectively.

3.2. Shadowing and σ_L/σ_T

A well-known prediction of the parton model is that DIS is dominated by the scattering of transverse photons, *i.e.*, $R = \sigma_L/\sigma_T = 0$ (the Callan-Gross relation). In the target rest frame picture (6) this is a consequence of the fact that only transverse photons readily split asymmetrically into $q\bar{q}$ pairs where one of the quarks carries wee momentum (see section 5.1). For the gluon scattering case (8) there is no similar restriction, hence $R = \mathcal{O}(\alpha_s)$. For scattering on nuclei, it is possible that shadowing affects σ_L differently from σ_T (*e.g.*, if the gluon structure function is more shadowed than the quark one [7, 8] or due to higher twist effects induced by Fermi motion [9]). The (scant) available data on the nuclear dependence of R in the shadowing region

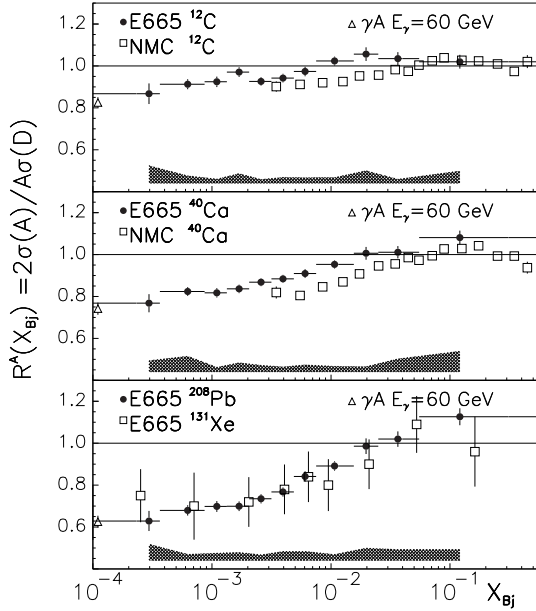


Figure 3. E665 [15] and NMC [12] data on shadowing in the structure function at low x .

suggests at most a small effect. An earlier NMC result $R^{Ca} - R^C = 0.027 \pm 0.026 \pm 0.020$ (for $.007 < x < .2$) was consistent with no effect. Preliminary data presented by the NMC at this meeting [11] shows a small positive result, $R^{Sn} - R^C = 0.031 \pm 0.017$, consistent with a larger shadowing for gluons.

3.3. Q^2 Dependence of Shadowing

In recent years, extensive data on nuclear structure functions in the shadowing region has been obtained in particular by the NMC [4, 12, 13] and E665 [14, 15] collaborations. The distributions extend to very low x as seen in figure 3 from Ref. [15].

When the nuclear DIS cross section is parameterized as $\sigma(\gamma^*A) = A^{\alpha(x)}\sigma(\gamma^*N)$, E665 finds [15] that the exponent $\alpha(x)$ decreases with x from $\alpha(0.05) \simeq 0$ to $\alpha(0.002) = 0.906 \pm 0.006$ and remains consistent with the latter value for $0.0003 \leq x \leq 0.002$.

The kinematics of the fixed target data is such that Q^2 decreases with x , with $\langle Q^2 \rangle \lesssim 0.5 \text{ GeV}^2$ for $x \leq 0.002$ in E665. Hence the data should join smoothly with the real photoproduction ($Q^2 = 0$) data for $x \rightarrow 0$, as is in fact observed in figure 3.

Due to the low values of Q^2 one might expect the shadowing effect to show some residual Q^2 dependence.

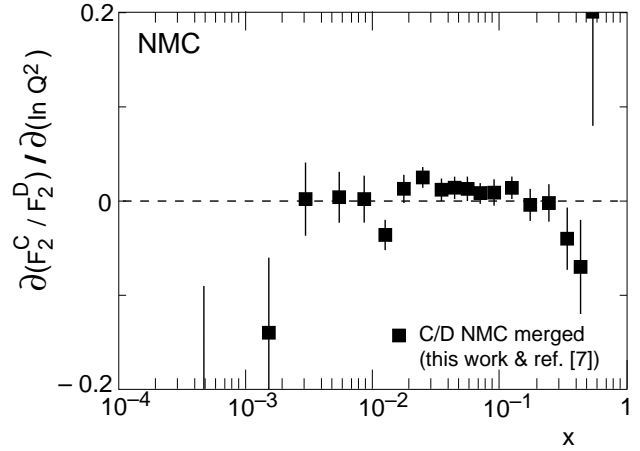


Figure 4. The dependence of F_2^C/F_2^D on $\log Q^2$ as measured by NMC [13].

The published NMC [12, 13] and E665 [15] data nevertheless shows that the shadowing is at most weakly dependent on Q^2 at fixed x , see figure 4.

3.4. Theoretical models of shadowing in DIS

Quantitative models for describing the shadowing effect, based on the target rest frame view outlined in section 3.1, have been constructed by several authors [6, 7, 16, 17, 18, 19]. In order to properly describe also the very small x , low Q^2 data the contribution of vector meson production has been taken into account. With plausible parametrizations of the $q\bar{q}$ cross section on nuclei the shadowing effect can be adequately described. The models [18, 19] give a somewhat larger Q^2 dependence for the shadowing effect than is observed in the present data. A prediction for the Q^2 dependence of the F_2^{Sn}/F_2^C ratio from Ref. [18] is shown in figure 5. The model of Ref. [19] gives a very similar prediction. Preliminary NMC data reported at this meeting [11] does indicate a positive Q^2 dependence for this ratio.

At very low values of x the parton densities of heavy nuclei can become large enough for parton recombination to occur in the Q^2 evolution [20]. This gives rise to another type of shadowing effect which is not, however, expected to be relevant in the x and Q^2 range of the present data.

An explanation of the 'anti-shadowing' nuclear enhancement effect observed for $0.1 \lesssim x \lesssim 0.2$ has been offered by Brodsky and Lu [16], who use a Regge model for $\bar{q}A$ scattering (recall that the \bar{q} momentum is of $\mathcal{O}(1/x)$ and hence large at low x). They find (with a suitable choice of the Regge parameters) that the enhancement can be understood as due to interference between the leading (Pomeron) and secondary (meson)

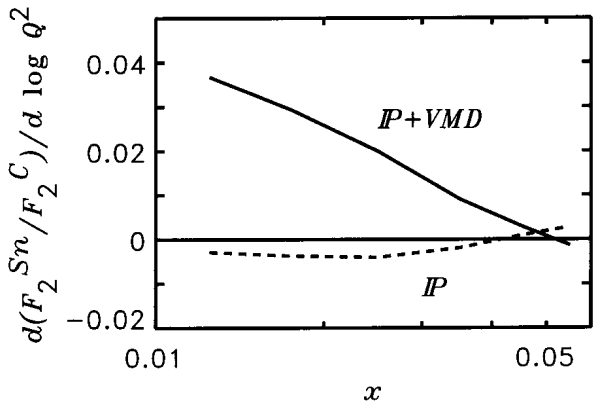


Figure 5. The dependence of F_2^{Sn}/F_2^C on $\log Q^2$ according to [18]. The solid curve is the full result, while the dashed one shows the Pomeron contribution only.

Regge exchanges.

It was recently proposed [21] that the shadowing effect should scale as a function of the number of gluons $n(x, Q^2, A)$ which interact with the $q\bar{q}$ fluctuation during its lifetime. This number was estimated as

$$n(x, Q^2, A) = \frac{\langle \sigma^2(\rho) \rangle}{4\langle \sigma(\rho) \rangle} \langle T(b) \rangle F_A^2(q) x^{-\Delta_P(Q^2)} \quad (9)$$

Here ρ is the transverse size of the $q\bar{q}$ pair, $\sigma(\rho, x) = \sigma(\rho) x^{-\Delta_P(Q^2)}$ is the interaction cross section of the quark pair with a nucleon, $T(b)$ is the nuclear density profile in impact parameter space and $F_A(q)$ is the nuclear longitudinal form factor. Assuming specific, physically motivated forms for the quantities appearing in Eq. (9), the scaling prediction seems to be in good agreement with the available data, as shown in figure 6.

3.5. Structure functions in configuration space

Due to the highly inclusive nature of DIS, the measurements provide only limited possibilities of testing detailed model assumptions. In view of this it is interesting to note that the structure functions can, in a model independent way, be studied also in coordinate space [22]. The coordinate and momentum space descriptions of the structure functions contain equivalent information and are related by a Fourier transform. For example, for the valence quark structure function the relation is

$$q_{val}(z, Q^2) = \int_0^1 dx \cos(xz) q_{val}(x, Q^2) \quad (10)$$

where x is the standard Bjorken energy fraction and $z = m_N L_I$ ($L_I =$ Ioffe length, see Eq. (4)) measures

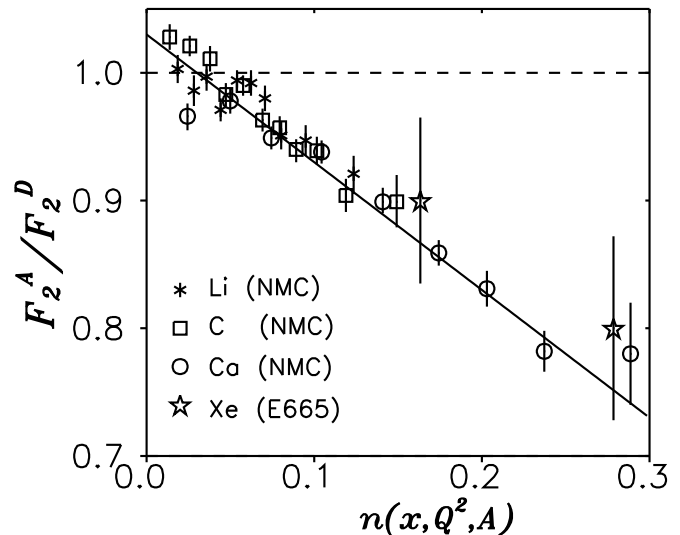


Figure 6. A scaling prediction of shadowing compared with data [21]. The scaling variable $n(x, Q^2, A)$ is defined by Eq. (9).

the longitudinal light cone size of the quark distribution. The Q^2 evolution of $q_{val}(z, Q^2)$ is given implicitly by Eq. (10) in terms of that for $q_{val}(x, Q^2)$. The Q^2 evolution equation can also be written directly in coordinate space.

It may be worthwhile to study the nuclear effects on the structure functions also in coordinate space. This will give a model independent characterization of how the spatial distribution of quarks in nucleons is modified in the nuclear environment.

4. Hadronization of the quark jet

In our discussion of the space-time picture of DIS, we noted that the photon splits asymmetrically into a $q\bar{q}$ pair, such that one of the quarks takes almost all the photon momentum. This quark (which is the final state struck quark in the infinite momentum frame picture) forms the ‘current jet’ of hadrons. For nuclear targets, the fast quark must first penetrate the nucleus. At sufficiently high hadron energy $E_h \gtrsim \mathcal{O}(R_A \langle p_\perp^2 \rangle)$, where $\langle p_\perp^2 \rangle$ is a hadronization energy scale of $\mathcal{O}(\Lambda_{QCD}^2)$, the hadronization will (due to time dilation) start only after the quark has penetrated the nucleus. The hadronization should then be *independent* of the target size A .

Note that there can be hard gluon emission at a short time scale inside the nucleus, when the quark is produced at high virtuality. Such emission is associated with the hard vertex and independent of the nuclear size. Furthermore, the quark is initially ‘bare’ (unaccompanied by soft gluon radiation) and at large ν

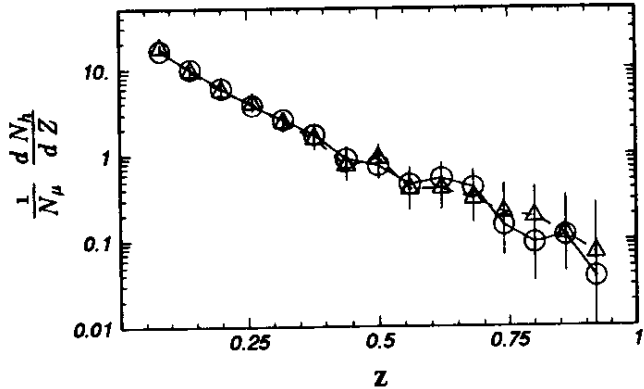


Figure 7. Hadron distributions in μA scattering [24] as a function of the hadron fractional laboratory energy $z = E_h/\nu$, for $A = D_2$ (circles) and $A = Xe$ (triangles). The events satisfy the constraints $x < 0.005$ and $Q^2 < 1 \text{ GeV}^2$, a kinematic region where a strong shadowing effect is observed in the DIS cross section.

has no time to form a soft gluon cloud while inside the nucleus. Hence there is no A -dependent energy loss [23], only elastic quark scattering as shown in figure 2.

The data agrees well with this simple picture. As an example, I show in figure 7 the 490 GeV μA data of E665 [24] on the inclusive hadron momentum spectrum in the current jet. The hadron distribution is plotted as a function of the fractional energy z that the hadron carries of the virtual photon energy ν . There is no observable difference between the distribution measured for a heavy target (Xe) compared to that for a light target (D_2), in the whole measured range $.05 \leq z \leq .95$. If the fast quark suffered energy loss in the nucleus one would, on the contrary, expect that the z -distribution for Xe would be steeper than that for D_2 . The data was interpreted [24] as an upper limit of 1.7 mb (90 % c.l.) for the effective nuclear rescattering cross section of the fast quark.

The data in figure 7 is selected for leptons scattered with $x < 0.005$ and $Q^2 < 1 \text{ GeV}^2$, *i.e.*, in the region where strong shadowing is observed in the DIS cross section. Very similar results were obtained [24] in the non-shadowing region $x > 0.03$ and $Q^2 > 2 \text{ GeV}^2$. Apparently, the shadowing (which naively might be interpreted as a hadronlike behavior of the virtual photon) does not influence in any way the (absence of) energy loss of the fast quark in the nucleus. This is what we should expect from the general space-time picture of DIS – whether the fast quark is produced in front of or inside the nucleus it has no time to form a soft gluon cloud before passing the nucleus.

The trivial A -dependence of the hadron distribution in DIS at high ν is important in that it establishes a

region where the nucleus behaves in a simple and well understood way. It shows that even colored particles can penetrate nuclear matter without energy loss, under proper conditions. Once this is established, one can turn to study the deviations which appear at low ν . The data [25, 26] shows that the production of hadrons with $z \geq 0.2$ is about 10% lower on heavy nuclei, compared to light targets, for $20 \lesssim \nu \lesssim 80 \text{ GeV}$. The data at still lower values of ν is limited to a data point from an early experiment at SLAC [27] with $\nu \simeq 10 \text{ GeV}$, which indicates a much stronger nuclear suppression than the higher ν data. More data in the $\nu \lesssim 30 \text{ GeV}$ region is needed to map out the effects of hadronization inside the nucleus.

Our theoretical understanding of energy loss and hadronization effects in a nuclear medium is still quite limited. The argument used above for a finite energy loss (hence vanishing fractional energy loss at high ν) is a direct consequence of the uncertainty principle [23]. Detailed studies of the energy loss in hot QCD matter have been made in [28, 29, 30]. In Ref. [29] it is concluded that the energy loss per unit distance (in an infinitely long medium) is actually proportional to the square root of the energy of the radiating quark or gluon.

Fits to the observed A -dependence of the hadron distribution [25, 26, 27] have been made in a string-inspired model [31, 32]. It was concluded that a good fit required two time scales in the model. At the ‘constituent time’ the first constituent of the hadron shows up, and at the ‘yo-yo time’ this constituent finds a partner and forms a color singlet hadron. In [33] it is pointed out that hadrons with a large fraction of the quark energy, $z \rightarrow 1$, are formed early but in a small configuration. In this regime the effects of color transparency thus become important.

5. Color Transparency in DIS

Nuclei are expected to be transparent to fast color singlet system that have a small transverse size [34]. This phenomenon of *color transparency* (CT) has been the subject of intense experimental and theoretical interest (see Ref. [35] for a recent comprehensive review). If the transverse size of the (typically $q\bar{q}$ or qqq) system is b , only gluon interactions with transverse momenta of $\mathcal{O}(1/b)$ can resolve its color charges, and the nuclear interaction cross section is expected to be of $\mathcal{O}(b^2)$. A necessary condition for observing CT is that the energy E of the compact object is large enough in the nuclear rest frame, so that its small size b remains frozen during nuclear traversal. The growth of the transverse size is limited by the transverse velocity $v_\perp = p_\perp/E \simeq 1/bE$.

5.1. Compact $q\bar{q}$ pairs in the photon

DIS provides important tests of CT because the preparation of a transversally compact $q\bar{q}$ object of high energy is particularly simple using photons. The square of the wave function of a $q\bar{q}$ fluctuation in a transversally polarized photon of virtuality Q^2 is [7]

$$W_T(\alpha, b) = \frac{6\alpha_{em}}{(2\pi)^2} e_q^2 \{ [1 - 2\alpha(1 - \alpha)] \epsilon^2 K_1(\epsilon b)^2 + m_q^2 K_0(\epsilon b)^2 \} \quad (11)$$

where α is the momentum fraction of the quark of charge ee_q and mass m_q , $\alpha_{em} = e^2/4\pi$ and b is the transverse size of the pair. $K_{0,1}$ are Bessel functions and

$$\epsilon^2 = m_q^2 + \alpha(1 - \alpha)Q^2. \quad (12)$$

For small z , $K_0(z) \sim -\log(z)$ and $K_1(z) \sim 1/z$, while for large z the Bessel functions are exponentially small. Thus it can be seen from Eq. (11) that the $q\bar{q}$ pair has transverse size $b \lesssim 1/\epsilon$. For momentum fractions α of $\mathcal{O}(1/2)$ this implies, according to the definition (12), that b is of $\mathcal{O}(1/m_q)$ or $\mathcal{O}(1/Q)$, whichever is smaller. This is the ‘gluon scattering regime’ of Eq. (8) that we deduced above (in the case $m_q = 0$) from the uncertainty principle.

In the ‘parton model regime’ of Eq. (6) we see that ϵ , and hence also $1/b$, does not grow with Q^2 . From Eq. (11) and the behavior of the K_1 Bessel function we observe that $W_T \propto 1/b^2$ for small ϵ . The scattering cross-section σ_T of the virtual transverse photon is obtained by multiplying W_T with the $q\bar{q}$ interaction probability $\sigma(b)$,

$$\sigma_T = \int_0^1 d\alpha \int d^2\vec{b} \sigma(b) W_T(\alpha, b). \quad (13)$$

With $\sigma(b) \propto b^2$ we find (for $m_q = 0$) that the parton model domain ($\alpha \lesssim \mathcal{O}(1/Q^2)$ or $1 - \alpha \lesssim \mathcal{O}(1/Q^2)$) gives a scaling contribution $\sigma_T \propto 1/Q^2$ [7, 8]. All $q\bar{q}$ sizes b contribute in this domain. There is no contribution from longitudinal photons, whose squared wave function [7]

$$W_L(\alpha, b) = \frac{6\alpha_{em}}{(2\pi)^2} e_q^2 4Q^2 \alpha^2 (1 - \alpha)^2 K_0(\epsilon b)^2 \quad (14)$$

vanishes for $\alpha \rightarrow 0, 1$.

The gluon scattering regime $\alpha(1 - \alpha) \gtrsim \mathcal{O}(1/Q^2)$ gives scaling contributions $\sigma_{L,T} \propto \alpha_s(Q^2)/Q^2$ for both transverse and longitudinal photons. The $1/Q^2$ suppression in this case is due to the restriction $b \lesssim \mathcal{O}(1/Q)$, while the factor $\alpha_s(Q^2)$ results from the hardness of the gluon interaction [8].

5.2. A -dependence of vector meson production

From Eqs. (11,14) we see that the transverse size of a heavy quark pair is $b = \mathcal{O}(1/m_q)$ at low Q^2 . Early tests

of CT were thus provided by the measurements [36, 37, 38] of J/ψ photoproduction on nuclei, $\gamma A \rightarrow J/\psi + X$. Parametrizing the nuclear target dependence as $\sigma \propto A^\alpha$, E691 [38] found $\alpha = 0.94 \pm 0.02 \pm 0.02$ in the incoherent region for $p_\perp^2 > 0.15 \text{ GeV}^2$. More recently, the NMC collaboration [39] measured $\alpha = 0.90 \pm 0.03$ for the incoherent elastic process $\gamma A \rightarrow J/\psi A$. These exponents are significantly larger than the $\alpha \simeq 2/3$ expected and observed [40] in the photoproduction of light vector mesons such as the ρ .

In the region of the coherent p_\perp^2 peak of J/ψ production, E691 [38] obtained $\alpha = 1.40 \pm 0.06 \pm 0.04$, while NMC [39] found $\alpha = 1.19 \pm 0.02$. Full transparency would imply $\sigma_{coh}(A, p_\perp) \propto A^2 \exp(-cA^{2/3} p_\perp^2)$ (c being a constant), resulting in $\alpha = 4/3$ for the p_\perp -integrated cross-section. There is thus rather convincing evidence that the compact photoproduced $c\bar{c}$ pairs have a small nuclear reinteraction cross section, as predicted by CT.

Further evidence for CT has recently come from the measurement by E665 [40] of $\gamma^* A \rightarrow \rho A$ as a function of the virtuality Q^2 of the photon, as shown in figure 8. The A -dependence of the incoherent process ($|t'| > 0.1 \text{ GeV}^2$) is seen to be a function of Q^2 . For nearly real photons, $\alpha(Q^2 = 0.212 \text{ GeV}^2) = 0.640 \pm 0.030$, close to $2/3$ as expected for a surface dominated soft process. At the highest measured average virtuality, $\alpha(Q^2 = 5.24 \text{ GeV}^2) = 0.893 \pm 0.092$, which is consistent with the value measured for elastic J/ψ production [38, 39]. The average value of the photon energy in this data is about 120 GeV. The nuclear dependence of ρ muoproduction has also been measured by the NMC Collaboration [41]. In a sample of events which included both coherent and incoherent scattering they observed an effective power $\alpha = 1.035 \pm 0.032$, with no significant difference between an average Q^2 of 3.9 GeV^2 and 9.6 GeV^2 . It should be noted that $x \simeq 0.05$ for the high Q^2 NMC data, corresponding to a Ioffe length (see Eq. (4)) $L_I = 1/2m_N x \simeq 2 \text{ fm}$. Hence a significant fraction of the $q\bar{q}$ pairs are formed inside the target nucleus, and this fraction is larger for heavier targets. The measured A -dependence may thus only partly reflect the CT effect. This caveat is somewhat less serious for the E665 data, for which $x \lesssim 0.03$.

5.3. Comparison with models for vector meson production

Elastic leptoproduction of vector mesons has been described using an effective Pomeron exchange model [42], in terms of a constituent quark picture [43] and using a perturbative two gluon exchange diagram [44, 45]. These approaches have many similarities, in particular they predict (for large Q^2) the dominance of longitudinally polarized vector mesons and a $1/Q^6$ dependence on the virtuality of the photon.

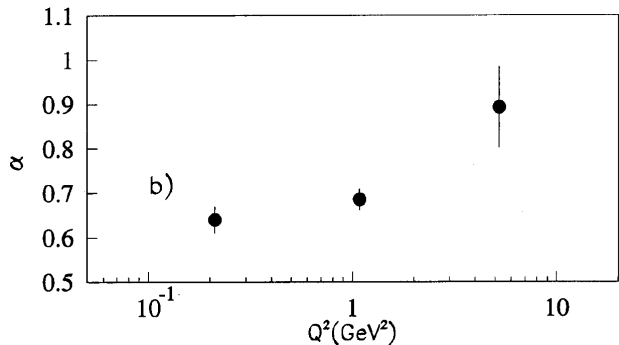


Figure 8. The effective exponent α of the nuclear target dependence in incoherent exclusive ρ muoproduction at 470 GeV [40], $\sigma(\mu A \rightarrow \mu \rho A) \propto A^\alpha$, as a function of the virtuality Q^2 of the photon.

The data is consistent with some increase with Q^2 of the longitudinal to transverse ρ production ratio, $R = \sigma_L/\sigma_T$. The NMC Collaboration obtained [41] $R = 2.0 \pm 0.3$ at $\langle Q^2 \rangle = 6 \text{ GeV}^2$, up from $R = -0.38 \pm 0.13_{-0.4}^{+0.9}$ at $Q^2 = 2 \text{ GeV}^2$ [46]. In the HERA energy range, the ZEUS Collaboration [47] measured $R = 1.5_{-0.6}^{+2.8}$ at $\langle Q^2 \rangle = 11 \text{ GeV}^2$.

If the Q^2 dependence of the ρ production cross section is parametrized as $1/Q^\beta$, the NMC Collaboration [41] obtains $\beta = 4.04 \pm 0.14$, with no significant difference between their deuterium, carbon and calcium targets. The ZEUS [47] data give $\beta = 4.2 \pm 0.8_{-0.5}^{+1.4}$. The data suggests that there are important corrections to the asymptotic $1/Q^6$ behavior expected in the model calculations, even in the HERA energy range.

The nuclear target A -dependence in the Pomeron exchange model would, under the most simple assumption of a factorizable Pomeron, be independent of Q^2 and of the quark mass, since these affect only the virtual photon vertex. As we have noted above, this is not consistent with the data (nor with CT). Hence, in a Pomeron exchange picture one is forced to distinguish between the ‘soft’ Pomeron, familiar from total cross sections and soft hadronic scattering, and a ‘hard’ Pomeron involved in short distance processes. The ‘hard’ Pomeron could in fact be nothing but two gluon exchange [44, 45], which has CT built into it and so is consistent with the A -dependence of the data, at least at a qualitative level.

The observed dependence of the vector meson cross section on the photon energy $\nu \simeq s/2m_p$ also demonstrates an important difference between hard and soft processes. The ZEUS data for ρ production from real photons [48] shows that the cross section increases only moderately with s , similarly to soft elastic hadron scattering and consistent with a ‘soft’ Pomeron intercept $\alpha_P(0) \simeq 1.08$. The large Q^2 ρ production cross section [47] as well as the J/ψ cross section [49] increases

much faster with s . In the gluon exchange model a fast increase is in fact expected. The cross section is (to leading order in $\log(1/x)$) predicted [44, 45] to be proportional to the square of the gluon structure function, $\sigma \propto [xG(x)]^2$, which increases rapidly at low $x \simeq Q^2/s$. The predicted s -dependence appears in fact to be somewhat too steep, but is consistent with the data given the considerable theoretical uncertainties [47, 49]. Combined with the observed discrepancy in the Q^2 -dependence, this may indicate that only one gluon is effectively hard in the present kinematic range [50].

It has been suggested [43] that studies of CT for the radial excitations of vector mesons (ρ', ψ') could reveal interesting behavior, including an *enhancement* of the nuclear production cross section, as compared to that on free nucleons. The production amplitude is proportional to the overlap of the $q\bar{q}$ wave function in the virtual photon, *cf.* Eqs. (11), (14), and that of the vector meson. The wave function of the radially excited states has a node, resulting in a cancellation in the overlap integral. The importance of the cancellation depends on Q^2 , which regulates the size of the $q\bar{q}$ pair in the photon. It is thus conceivable that for a suitable value of Q^2 the cancellation is almost complete for ρ' production on free nucleons. Nuclear targets modify the initial $q\bar{q}$ distribution by filtering out large pairs due to rescattering in the nucleus. This could upset the cancellation and result in a larger cross section.

More generally, the data on inclusive hadroproduction of J/ψ and ψ' illustrates the importance of studying the radially excited states. There are very considerable discrepancies [51] (up to a factor of 50) between the measured charmonium cross sections and the QCD calculations. Nevertheless, the ratio of the ψ' to J/ψ cross sections is consistent with being universal [52] for all beams, targets and reaction kinematics (with the exception [53] of nucleus-nucleus collisions). The measured cross section ratio is $\sigma(\psi')/\sigma_{dir}(J/\psi) \simeq .24 \pm .05$ for πN and pN collisions, and appears to be independent of the target size A^\dagger . This value is consistent with expectations based on the J/ψ and ψ' wave functions at the origin. This suggests that the size of the produced $c\bar{c}$ pair is small compared to the J/ψ and ψ' wave functions, and that there is little rescattering of the fully formed charmonium mesons.

The ψ' to J/ψ inclusive cross section ratio has also been measured in muoproduction off the (concrete) absorber in the NMC experiment [39]. The result, $\sigma(\psi')/\sigma(J/\psi) = 0.20 \pm .05 \pm 0.07$ can be directly compared with the ratio quoted above, since the production of χ_c states from photons should be

[†] For production on heavy nuclei the fraction of directly produced J/ψ 's (*i.e.*, those not originating from χ_c decays) has not been measured, and is assumed to be the same as that measured on nucleon targets.

suppressed. The fact that the ratios are consistent indicates that the A -dependence of the ψ' is similar to that of the J/ψ also in photon induced processes, *i.e.*, the enhancement scenario [43] apparently does not apply for the charmonium states.

5.4. Compact qqq configurations in the nucleus

A complementary way of investigating CT effects is to select compact objects in the nucleus itself, typically through hard exclusive scattering [34]. For example, in elastic $ep \rightarrow ep$ scattering at large momentum transfer Q^2 it is expected [54] that the only Fock components of the target proton which contribute are those whose transverse size is of $\mathcal{O}(1/Q)$. This follows from general arguments – the exchanged photon should scatter coherently over the whole target to avoid a breakup. By performing the reaction inside a nucleus one hopes to use the nucleus as a detector to directly measure the size of the scatterer as it recoils through the nucleus.

It should be noted that at finite energies the contributing Fock states are not necessarily compact. There is a competing mechanism, the ‘Feynman’ process [55], where the initial Fock state has one quark carrying a large momentum fraction $x \sim 1 - 1/Q^2$. The electron scatters on this quark only, while the remaining soft quarks reassociate themselves with the fast one after the hard scattering so as to form an intact proton moving in the new direction. Such Fock states can have a large transverse size of $\mathcal{O}(1 \text{ fm})$, which would upset the CT argument. The importance of this mechanism at finite Q^2 depends on the proton wave function. It is, however, believed to be subleading at asymptotic energies due to the Sudakov form factor of the fast quark [56]. The form factor expresses the small probability that a colored object, when given a big momentum transfer, will emit no gluon radiation, which would imply a breakup of the proton.

An early indication for a CT effect in large Q^2 quasielastic pp scattering was obtained from a study of the process $pA \rightarrow pp(A-1)$ at BNL [57]. Protons of momenta 6, 10 and 12 GeV/c scattered at $\theta_{cm}^{pp} = 90^\circ$ from H , Li , C , Al , Ca and Pb , with the kinematics constrained to correspond to elastic pp scattering and with no extra particle produced. The nuclear transparency, defined as

$$T = \frac{(d\sigma/dt)(pp \text{ elastic in nucleus})}{(d\sigma/dt)(pp \text{ elastic in hydrogen})} \quad (15)$$

was found to increase with beam momentum until about 10 GeV/c, but then fell abruptly. In comparison, no energy dependence is expected from a standard Glauber model calculation, where the struck proton reinteracts with the usual pN cross section. While the rise of

T at lower momenta thus could be a sign of CT, the interpretation of its decrease above 10 GeV/c is still under debate. Brodsky and de Teramond [58] have linked this behavior to the rapid energy dependence seen in the polarization parameter A_{NN} of pp elastic scattering. They suggest that both phenomena are due to the $c\bar{c}$ threshold, which can have a sizable influence on the small 90° cross section. Close to threshold the charm quarks have low momenta and hence a large transverse size. Ralston and Pire [59] observe from the measured energy dependence of large angle pp elastic scattering that the protons may at the relevant energies still have a large transverse size component due to the Landshoff mechanism [60] of three independent quark-quark scatterings. For scattering in the nucleus the large proton components would be filtered away, and thus they argue that the behavior of T is due to the behavior of the denominator rather than of the numerator of Eq. (15).

A better understanding of the puzzling energy dependence of the transparency T in pp scattering apparently requires data at higher energies. If the decrease in T is due to charm threshold, the transparency should be rapidly restored as the energy is increased, and remain large until the $b\bar{b}$ threshold is reached. The Ralston and Pire mechanism, on the other hand, predicts that the transparency has an oscillating behavior with energy.

More recently, the NE18 experiment [61] studied CT effects in the $eA \rightarrow ep(A-1)$ process. The energy of the beam electron was 2...5 GeV, Q^2 ranged from 1 to 6.8 GeV² and the targets used were 2H , C , Fe and Au . The invariant momentum transfer and the recoil proton energy were thus similar to (although slightly lower than) in the pp experiment [57]. NE18 defined the transparency as the ratio of the measured cross section with that estimated using a Plane Wave Impulse Approximation (PWIA), which neglects any final state interactions of the struck proton in the nucleus. Effects of the off-shellness and Fermi momentum of the struck nucleon were included in the PWIA calculation. The measured transparency was consistent with being independent of Q^2 for all targets (see figure 9 for $A = C$). The A -dependence of the transparency was consistent with a Glauber model calculation. The data thus gave no positive evidence for a CT effect.

Early theoretical estimates [62] suggested the possibility of seeing a modest CT effect. The result of several calculations is compared [35] with the NE18 data in figure 9. As may be seen, the difference between calculations which include a CT effect (CSE, GJM) and those without it (DWIA) is marginal. Given the model dependence of the calculations, no firm conclusions can be drawn. In particular, the same CT models can fit

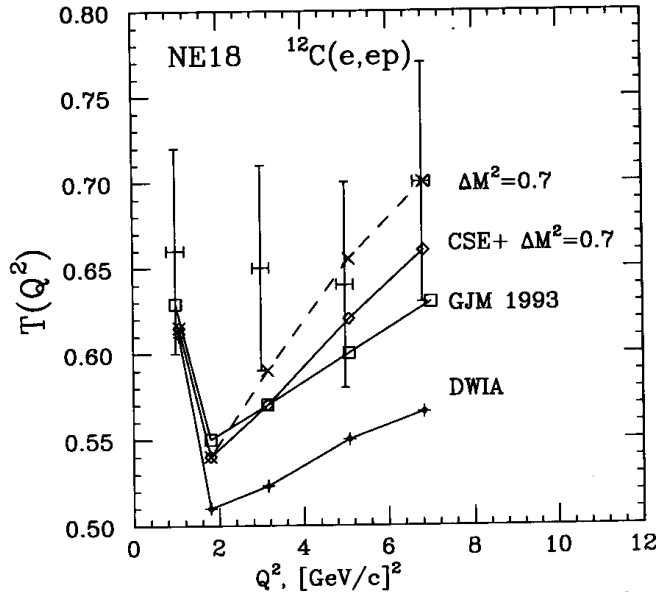


Figure 9. Nuclear transparency as measured by NE18 [61] in quasielastic electron scattering on nuclei, $eA \rightarrow ep(A-1)$. The data (error bars) is compared [35] with calculations including the effects of color transparency (CSE, GJM) and with a Glauber calculation (DWIA). Note the suppressed origin on the vertical axis.

both the BNL [57] and NE18 [61] data.

5.5. Comparison of the two types of CT test

Although the values of Q^2 were similar, there are important differences between the two types of CT test discussed above in sections 5.2 and 5.4.

- *Kinematics.* The vector mesons ($J/\psi, \rho$) were produced with energies ν of $\mathcal{O}(100 \text{ GeV})$ [38, 39, 40] and therefore had little time to expand before leaving the nucleus. By contrast, the recoil protons in the BNL [57] and NE18 [61] experiments had energies of $\mathcal{O}(5 \text{ GeV})$ or less. Hence, their transverse expansion within the nucleus must be modelled, and any CT effects are diminished.
- *Selection of compact systems.* In the case of vector meson production, the creation of a compact $q\bar{q}$ pair from the virtual photon is rather well understood – it is governed by the photon wave function of Eqs. (11), (14). On the other hand, as briefly discussed above, in large angle elastic scattering on nuclei the size distribution of the contributing proton Fock states for a given Q^2 is uncertain.
- *A-dependence of Fock state probabilities.* The probability distribution of compact $q\bar{q}$ pairs in the photon is, as noted above, governed by the photon wave function and thus independent of the target

size A . However, it is not as obvious that the probability of finding compact qqq states in the nucleus is independent of the nuclear size. In the CT analysis it must be assumed that this probability is the same as that for free nucleons. One nucleon shrinks to a small size without the rest of the nucleons noticing. Nevertheless, properties like the shell structure of the nucleus must be quite different for the shortlived fluctuations. It is in principle impossible to determine to which nuclear energy shell the struck system belonged – its lifetime $1/Q$ is so short that the uncertainty in its energy far exceeds the energy spread of the shell structure (see, however, Ref. [63]). The contributions from nucleons on all shells should be added coherently. Moreover, it is not even necessary that the qqq system originates from a single nucleon – compact states might be formed through the overlap of two or more normal sized nucleons.

6. High momentum densities in nuclei

The study of hard exclusive scattering in nuclei is part of an extensive but still poorly understood area of short distance correlations in nuclei. At some (low) level of probability, nuclei have dense Fock components, in which some or all of the quarks and gluons are packed into a small volume. Such nuclear configurations may have lost much of their nucleon substructure, *i.e.*, they do not consist of A color neutral qqq subsystems, but can display normally hidden color degrees of freedom. The dense subsystems give rise to effects which are kinematically forbidden for scattering on single nucleons.

6.1. Subthreshold production

The cross section near threshold for particle production on nuclei gives an indication of the effective mass and momentum of the subsystem in the target on which the projectile scatters. Thus, while the threshold for antiproton production on free nucleons at rest, $p + p \rightarrow \bar{p} + X$, is $E_{proj} \simeq 6.6 \text{ GeV}$, the same reaction has been measured on a copper target, $p + Cu \rightarrow \bar{p} + X$ down to $E_{proj} \lesssim 3.0 \text{ GeV}$ [64]. If the scattering occurred on single nucleons in the copper nucleus, this would imply Fermi momenta of more than 750 MeV. However, such a description turns out not to be selfconsistent. Modelling the nucleon motion by a sufficiently broad Fermi distribution, such that the $p + Cu$ data could be fitted, resulted [64] in an underestimate by a factor of 1000 for the nucleus-nucleus process $Si + Si \rightarrow \bar{p} + X$ at $E_{proj}/A \simeq 2.1 \text{ GeV}$. Subthreshold production thus appears to involve scattering on dense subsystems of nucleons or partons, rather than on normal nucleons.

6.2. Cumulative production

It has long been known [65] that in the scattering of various projectiles on nuclei, hadrons are produced in the backward direction with momenta that far exceed the kinematic limit for scattering on single nucleons at rest. The measured values of the lightcone energy fraction in the target rest frame for hadrons produced near 180° , $x = (E - p_L)/m_A$, reach up to values of $x \simeq 4$ for protons in pA collisions [66], suggesting that at least four nucleons in the nucleus have been involved in the scattering. These cumulative phenomena are only weakly dependent on the projectile type and energy, having been observed for hadron, photon, neutrino and nuclear projectiles of momenta from 1 to 400 GeV. This strongly suggests that the cumulative phenomena are related to the nuclear target wave function. In $A_p A_t$ nucleus-nucleus collisions the dependence of the cumulative cross section on the atomic number of the projectile A_p and target A_t has been found [67] to scale like $A_p^{2/3} A_t^{4/3}$, consistent with a soft (surface dominated) projectile scattering but a faster than volume increase with the target size. There is evidence [66] that the backward produced hadrons have large transverse momenta, suggesting that they originate from a target subsystem of small transverse size.

6.3. DIS at $x \gtrsim 1$

A direct way of observing phenomena that only can occur in nuclei is DIS at $x > 1$. Present data [68] at the largest $x \simeq 2$ is limited to low values of the photon energy $\nu = \mathcal{O}(300 \dots 500 \text{ MeV})$, and is thus not really in the ‘deep inelastic’ region. Nevertheless, various scaling phenomena have been studied [69]. For $x \simeq 1$ and $Q^2 \lesssim 3 \text{ GeV}^2$ the reaction is quasielastic, and scaling is observed in a variable y related to the Fermi motion of the struck nucleon. The y -scaling is found [70] to break down at higher values of Q^2 , where the scattering becomes inelastic and presumably occurs off quarks rather than nucleons. As shown in figure 10 a rough scaling in the whole Q^2 range is, however, observed in terms of the Nachtmann scaling variable $\xi = 2x/[1 + (1 + 4m_p^2 x^2/Q^2)^{1/2}]$ (which takes into account target mass effects), suggesting a duality between the quasielastic and inelastic processes.

The behavior of hard QCD processes at large values of x , where higher twist processes dominate and several partons scatter coherently, have been studied qualitatively in Ref. [71]. The general features agree with what is observed, *e.g.*, in the cumulative process of backward hadron production. In particular, the scattering of the projectile becomes softer, since it occurs off the soft stopped partons that contributed their momenta to the large x subsystem.

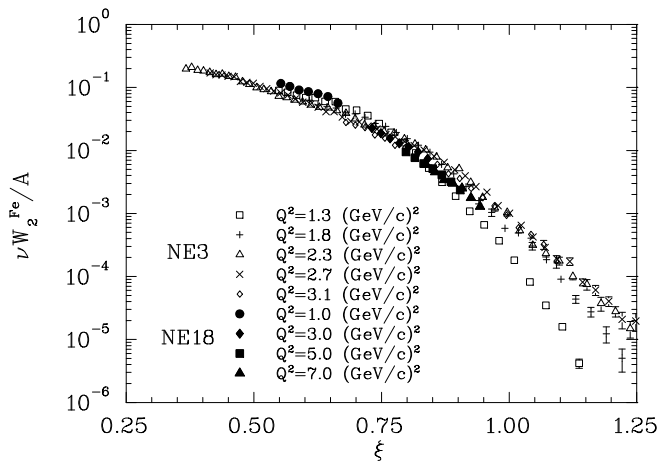


Figure 10. νW_2^{Fe} as measured at large x by the NE3 and NE18 experiments [70], shown as a function of the Nachtmann scaling variable ξ for a range of Q^2 values.

7. Summary

This presentation has perforce covered only a minor part of the rich phenomena that occur in scattering on nuclei, and the selection has been heavily influenced by my own limited knowledge of the field. Nevertheless, I am convinced that light can be thrown on many fundamental questions through DIS on nuclei. Here ‘DIS’ is taken to mean not only the fully inclusive process $eA \rightarrow eX$, but more generally hard scattering on nuclei initiated by real or virtual photons. The topics can be roughly divided into two classes.

- *Space-time development of hard scattering.* Secondary (soft) scattering in the extended nucleus gives information about the development of the partonic subsystems before and after the hard scattering. The nucleus acts as a ‘femtovertex’ detector. The *shadowing* of DIS at small x indicates the transverse size of the system formed by the virtual photon. The (absence of) *energy loss* of the fast quark produced by the virtual photon shows the slow development of hadronization. The *color transparency* observed in the production of J/ψ and ρ mesons indicates that the quark pairs created by highly virtual photons have a small size compared to the confinement scale.
- *Short-range correlations in nuclei.* Perturbative QCD should correctly describe phenomena taking place over distances $\ll 1 \text{ fm}$. Nuclei provide an extensive testing ground for the theory, and can give us valuable insights into the applicability of QCD. The experimental signals of *subthreshold production*, *cumulative processes* and *DIS at $x > 1$* are still poorly understood theoretically. High sensitivity

experiments are needed to properly study the rare Fock states of nuclei.

Real and virtual photons are the most precise tools we have for exploring the fine structure of matter. It is very important that they can be brought to bear also on nuclear targets. With facilities such as CEBAF, HERMES and ELFE the future prospects look promising.

Acknowledgements

It is a pleasure to thank the organizing committee for inviting me to present this review. I have benefitted from discussions on hard scattering in nuclei with many colleagues, and in particular with Stan Brodsky, Boris Kopeliovich, Mark Strikman, Wai-Keung Tang, Ramona Vogt and Mikko Vanttinen.

References

- [1] J. J. Aubert *et al* (EMC), Phys. Lett. B123 (1983) 275.
- [2] M. Arneodo, Phys. Rep. 240 (1994) 301.
- [3] J. Gomez *et al* (E139), Phys. Rev. D49 (1994) 4348.
- [4] P. Amaudruz *et al* (NMC), to be published in Nucl. Phys. (hep-ph/9503291).
- [5] V. N. Gribov, B. L. Ioffe and I. Ya. Pomeranchuk, Yad. Fiz. 2 (1965) 768; B. L. Ioffe, Phys. Lett. B30 (1968) 123.
- [6] J. D. Bjorken and J. Kogut, Phys. Rev. 28 (1973) 1341; N. N. Nikolaev and V. I. Zakharov, Phys. Lett. B55 (1975) 397; Th. Baier, R. D. Spital, D. K. Yennie and F. M. Pipkin, Rev. Mod. Phys. 50 (1978) 261; L. L. Frankfurt and M. I. Strikman, Nucl. Phys. B316 (1989) 340.
- [7] N. N. Nikolaev and V. I. Zakharov, Z. Phys. C49 (1991) 607.
- [8] V. Del Duca, S. J. Brodsky and P. Hoyer, Phys. Rev. D46 (1992) 931.
- [9] J. Milana, Phys. Rev. C49 (1994) 2820 (hep-ph/9309328).
- [10] P. Amaudruz *et al* (NMC), Phys. Lett. B294 (1992) 120.
- [11] A. Mücklich (NMC), Contribution to this meeting.
- [12] P. Amaudruz *et al* (NMC), Z. Phys. C51 (1991) 387; Phys. Lett. B295 (1992) 159; Nucl. Phys. B441 (1995) 3; M. Arneodo *et al* (NMC), Nuovo Cim. 107A (1994) 2141.
- [13] M. Arneodo *et al* (NMC), CERN PPE 95-32 (hep-ex/9504002).
- [14] M. R. Adams *et al* (E665), Phys. Rev. Lett. 68 (1992) 3266; Phys. Lett. B287 (1992) 375; B309 (1993) 477.
- [15] M. R. Adams *et al* (E665), Fermilab preprint (April 1995) (hep-ex/9505006).
- [16] S. J. Brodsky and H. J. Lu, Phys. Rev. Lett. 64 (1990) 1342.
- [17] B. Badelek and J. Kwieciński, Nucl. Phys. B370 (1992) 278.
- [18] W. Melnitchouk and A. W. Thomas, Phys. Lett. B317 (1993) 437; preprint ADP-95-31/T185 (hep-ph/9508311).
- [19] S. A. Kulagin, G. Piller and W. Weise, Phys. Rev. C50 (1994) 1154; G. Piller, W. Ratzka and W. Weise, preprint ADP-95-10/T173 (to be published in Z. Phys. A) (hep-ph/9504407).
- [20] A. H. Mueller and J. Qiu, Nucl. Phys. B268 (1986) 427; J. Qiu, Nucl. Phys. B291 (1987) 746; L. McLerran and R. Venugopalan, Phys. Rev. D49 (1994) 2233 and 3352; D50 (1994) 2225.
- [21] B. Kopeliovich and B. Povh, Heidelberg preprint MPIH-V12-1995 (hep-ph/9504380).
- [22] V. Braun, P. Górnicki and L. Mankiewicz, Phys. Rev. D51 (1995) 6036 (hep-ph/9410318).
- [23] S. J. Brodsky and P. Hoyer, Phys. Lett. B298 (1993) 165.
- [24] M. R. Adams *et al* (E665), Phys. Rev. D50 (1994) 1836.
- [25] J. Ashman *et al* (NA2), Z. Phys. C52 (1991) 1.
- [26] A. F. Salvarani (E665), PhD Thesis Univ. Calif. San Diego (1991); W. Busza, Nucl. Phys. A544 (1992) 49.
- [27] L. S. Osborne *et al*, Phys. Rev. Lett. 40 (1978) 1624.
- [28] M. Gyulassy and X.-N. Wang, Nucl. Phys. B420 (1994) 583; X.-N. Wang, M. Gyulassy and M. Plümer, Phys. Rev. D51 (1995) 3436 (hep-ph/9408344).
- [29] R. Baier, Yu. L. Dokshitzer, S. Peigné and D. Schiff, Phys. Lett. B345 (1995) 277 (hep-ph/9411409); D. Schiff, contribution to this meeting.
- [30] E. Levin, preprint CBPF-NF-061/95 (hep-ph/9508414).
- [31] A. Białas and M. Gyulassy, Nucl. Phys. B291 (1987) 793; A. Białas and J. Czyżewski, Phys. Lett. B222 (1989) 132.
- [32] M. Gyulassy and M. Plümer, Nucl. Phys. B346 (1990) 1.
- [33] B. Z. Kopeliovich and J. Nemchik, SANITA preprint INFN-ISS 91/3 (1991); B. Kopeliovich, in BNL Future Direct. (1993) 60 (QCD161:W587:1993) (hep-ph/9305256).
- [34] S. J. Brodsky and A. H. Mueller, Phys. Lett. B206 (1988) 685; L. Frankfurt and M. Strikman, Phys. Rep. 160 (1988) 235.
- [35] L. L. Frankfurt, G. A. Miller and M. Strikman, Ann. Rev. Nucl. Part. Sci. 45 (1994) 501.
- [36] R. L. Anderson *et al*, Phys. Rev. Lett. 38 (1977) 263.
- [37] J. J. Aubert *et al* (EMC), Phys. Lett. 152B (1985) 433.
- [38] M. D. Sokoloff *et al* (E691), Phys. Rev. Lett. 57 (1986) 3003.
- [39] P. Amaudruz *et al* (NMC), Nucl. Phys. 371 (1992) 553.
- [40] M. R. Adams *et al* (E665), Phys. Rev. Lett. 74 (1995) 1525.
- [41] M. Arneodo *et al* (NMC), Nucl. Phys. B429 (1994) 503.
- [42] A. Donnachie and P. V. Landshoff, Phys. Lett. 185B (1987) 403; Nucl. Phys. B311 (1989) 509.
- [43] B. Z. Kopeliovich, J. Nemchik, N. N. Nikolaev and B. G. Zakharov, Phys. Lett. B309 (1993) 179 (hep-ph/9305225); Phys. Lett. B324 (1994) 469 (hep-ph/9311237).
- [44] M. G. Ryskin, Z. Phys. C57 (1993) 89.
- [45] S. J. Brodsky, L. Frankfurt, J. F. Gunion, A. H. Mueller and M. Strikman, Phys. Rev. D50 (1994) 3134 (hep-ph/9402283).
- [46] J. J. Aubert *et al* (EMC), Phys. Lett. B161 (1985) 203.
- [47] M. Derrick *et al* (ZEUS), preprint DESY 95-133 (hep-ex/9507001).
- [48] M. Derrick *et al* (ZEUS), preprint DESY 95-143 (hep-ex/9507011).
- [49] M. Derrick *et al* (ZEUS), Phys. Lett. B350 (1995) 120 (hep-ex/9503015).
- [50] P. Hoyer and C. S. Lam, preprint NORDITA 95/53 P, to be published in Z. Phys. C (hep-ph/9507367).
- [51] V. Papadimitriou (CDF), Talk at the XXXth Rencontres de Moriond, March 1995, Fermilab-Conf-95/123-E.
- [52] M. Vanttinen, P. Hoyer, S. J. Brodsky and W.-K. Tang, Phys. Rev. D51 (1995) 3332; R. Gavaï, D. Kharzeev, H. Satz, G. A. Schuler, K. Sridhar and R. Vogt, preprint CERN-TH.7526/94 (hep-ph/9502270).
- [53] M. C. Abreu *et al* (NA38), Nucl. Phys. A566 (1994) 371c.
- [54] S. J. Brodsky and G. P. Lepage, Phys. Rev. D22 (1980) 2157; A. H. Mueller, Phys. Rep. 73 (1981) 237.
- [55] R. P. Feynman, *Photon-Hadron Interactions*, Reading: Benjamin (1972); A. V. Radyushkin, Acta Phys. Polon. B15 (1984) 403; N. Isgur and C. H. Llewellyn-Smith, Phys.

- Rev. Lett. 52 (1984) 1080; Phys. Lett. B217 (1989) 535.
- [56] J. Botts and G. Sterman, Nucl. Phys. B325 (1989) 62.
 - [57] R. S. Carroll *et al* , Phys. Rev. Lett. 61 (1988) 1698.
 - [58] S. J. Brodsky and G. F. de Teramond, Phys. Rev. Lett. 60 (1988) 1924.
 - [59] J. P. Ralston and B. Pire, Phys. Rev. Lett. 61 (1988) 1823.
 - [60] P. Landshoff, Phys. Rev. D10 (1974) 1024.
 - [61] N. C. R. Makins *et al* (NE18), Phys. Rev. Lett. 72 (1994) 1986; T. G. O'Neill *et al* (NE18), Phys. Lett. B351 (1995) 87.
 - [62] G. Farrar, H. Liu, L. L. Frankfurt and M. I. Strikman, Phys. Rev. Lett. 61 (1988) 686; O. Benhar *et al* , Phys. Rev. Lett. 69 (1992) 881; B. K. Jennings and G. A. Miller, Phys. Rev. Lett. 69 (1992) 3619.
 - [63] L. L. Frankfurt, E. J. Moniz, M. M. Sargsyan and M. I. Strikman, Phys. Rev. C51 (1995) 3435 (nucl-th/9501019).
 - [64] J. B. Carroll *et al* , Phys. Rev. Lett. 62 (1989) 1829.
 - [65] V. S. Stavinskii, Sov. J. Part. Nucl. 10 (1979) 373; L. Frankfurt and M. Strikman, Phys. Rep. 160 (1988) 235.
 - [66] S. V. Boyarinov *et al* , Sov. J. Nucl. Phys. 46 (1987) 871.
 - [67] J. V. Geagea *et al* , Phys. Rev. Lett. 45 (1980) 1993.
 - [68] D. B. Day *et al* , Phys. Rev. C48 (1993) 1849.
 - [69] L. L. Frankfurt, M. I. Strikman, D. B. Day and M. M. Sargsyan, Phys. Rev. C48 (1993) 2451.
 - [70] J. Arrington *et al* , preprint (nucl-ex/9504003).
 - [71] S. J. Brodsky, P. Hoyer, A. H. Mueller and W.-K. Tang, Nucl. Phys. B369 (1992) 519.